

Video Article

Generation and Control of Electrohydrodynamic Flows in Aqueous Electrolyte Solutions

Kentaro Doi¹, Fumika Nito¹, Ayako Yano², Ryo Nagura¹, Satoyuki Kawano¹

¹Department of Mechanical Science and Bioengineering, Graduate School of Engineering Science, Osaka University

²Division of Mechanical Science and Technology, Faculty of Science and Technology, GUNMA University

Correspondence to: Kentaro Doi at doi@me.es.osaka-u.ac.jp, Satoyuki Kawano at kawano@me.es.osaka-u.ac.jp

URL: <https://www.jove.com/video/57820>

DOI: [doi:10.3791/57820](https://doi.org/10.3791/57820)

Keywords: Engineering, Issue 139, Electrohydrodynamic flow, ionic current, aqueous solution, rectification, electrophoresis, ion-exchange membrane

Date Published: 9/7/2018

Citation: Doi, K., Nito, F., Yano, A., Nagura, R., Kawano, S. Generation and Control of Electrohydrodynamic Flows in Aqueous Electrolyte Solutions. *J. Vis. Exp.* (139), e57820, doi:10.3791/57820 (2018).

Abstract

To drive electrohydrodynamic (EHD) flows in aqueous solutions, the separation of cation and anion transport pathways is essential because a directed electric body force has to be induced by ionic motions in liquid. On the other hand, positive and negative charges attract each other, and electroneutrality is maintained everywhere in equilibrium conditions. Furthermore, an increase in an applied voltage has to be suppressed to avoid water electrolysis, which causes the solutions to become unstable. Usually, EHD flows can be induced in non-aqueous solutions by applying extremely high voltages, such as tens of kV, to inject electrical charges. In this study, two methods are introduced to generate EHD flows induced by electrical charge separations in aqueous solutions, where two liquid phases are separated by an ion-exchange membrane. Due to a difference in the ionic mobility in the membrane, ion concentration polarization is induced between both sides of the membrane. In this study, we demonstrate two methods. (i) The relaxation of ion concentration gradients occurs via a flow channel that penetrates an ion-exchange membrane, where the transport of the slower species in the membrane selectively becomes dominant in the flow channel. This is a driving force to generate an EHD flow in the liquid. (ii) A long waiting time for the diffusion of ions passing through the ion-exchange membrane enables the generation of an ion-dragged flow by externally applying an electric field. Ions concentrated in a flow channel of a $1 \times 1 \text{ mm}^2$ cross-section determine the direction of the liquid flow, corresponding to the electrophoretic transport pathways. In both methods, the electric voltage difference required for an EHD flow generation is drastically reduced to near 2 V by rectifying the ion transport pathways.

Video Link

The video component of this article can be found at <https://www.jove.com/video/57820/>

Introduction

Recently, liquid flow control techniques have attracted much attention because of interest in the applications of micro- and nanofluidic devices^{1,2,3,4,5,6,7,8,9,10,11,12,13,14,15}. In polar solutions, such as aqueous solutions and ionic liquids, ions and electrically charged particles usually bring about electrical charges in liquid flows. The transport of such polarized particles provides an expansion of various applications, such as single-molecule manipulation^{6,10,11,13,14,15,16,17}, ion diode devices^{12,18}, and liquid flow control^{19,20,21,22}. EHD flow has been an applicable phenomenon for liquid flow control systems since Stuetzer^{1,2} invented the ion drag pump. Melcher and Taylor³ published an important article in which the theoretical framework of EHD flow was well reviewed and some outstanding experiments were also demonstrated. Saville⁴ and his coworkers^{23,24} contributed to the following expansion of EHD technologies in liquids. However, there were some limitations to inducing liquid flows driven by electric forces, because tens of kV have to be applied in liquids to inject electrical charges in non-polar solutions, such as oils, to polarize them^{1,2,3}. This is a disadvantage for aqueous solutions because the water electrolysis that is induced by an electric potential higher than 1.23 V changes the characteristics of solutions and makes the solutions unstable.

In micro- and nanofluidic channels, surface charges of channel walls cause the concentration of counterions that effectively induce electroosmotic flows (EOFs) under externally applied electric fields^{25,26,27,28,29}. Using EOFs, some liquid pumping techniques have been applied in aqueous solutions, reducing the electric voltages^{30,31,32}. On the other hand, EOFs are limited to being generated in micro- and nanospaces in which surface areas become more dominant than liquid volumes. Furthermore, depending on the transport of highly concentrated ions very near the wall surfaces, such as in electric double layers, the slip boundary only causes the liquid flow, which may not be sufficient to make pressure gradients^{7,8,22,26,27}. Fine tuning, such as to channel dimensions and salt concentrations, is required for the applications of EOF. In contrast, EHD flows driven by body forces seem to be available to transport masses and energies if the application voltages can be reduced to avoid degrading solvents. Recently, some researchers have suggested applications of EHD flows with low voltages^{33,34,35,36}. Although these technologies have not yet been implemented, the frontiers are expected to expand.

In previous studies, we also conducted experimental and theoretical work on EHD flows in aqueous solutions^{37,38,39,40}. It was supposed that the rectification of ion transport pathways was effective to generate electrically charged solutions that cause electric body forces under electric fields. By using an ion-exchange membrane and a flow channel crossing the membrane, we were able to rectify ionic currents. When applying an

anion-exchange membrane, cations concentrated in the flow channel dragged the solvents and developed an EHD flow^{37,38,39}. A difference in the mobility of ion species was an important factor when separating the cationic and anionic currents. Ion-exchange membranes effectively worked to modulate the mobility due to the ion selectivity. Ion transport phenomena were also investigated from the viewpoint of ionic current density influenced by applied electric fields⁴¹. These studies have been fruitful for developing manipulation techniques for single molecules, namely, micro- and nanoparticles, whose motions are strongly affected by thermal fluctuations^{11,16,17}. EOFs and EHD flows are expected to expand the variety of precise flow control methods as well as pressure gradients.

In this study, we demonstrate two methods to drive EHD flows in aqueous solutions. First, an NaOH solution is used for a working fluid to drive an EHD flow^{37,38,39}. An anion-exchange membrane separates the liquid into two parts. A polydimethylsiloxane (PDMS) flow channel with a cross-section of 1 x 1 mm and a length of 3 mm penetrates the membrane. By applying an electric potential of 2.2 V, the electrophoretic transport of Na⁺, H⁺, and OH⁻ ions is induced along the electric fields. An anion-exchange membrane and a flow channel effectively work to separate the ion transport pathways, where anions dominantly pass through the membrane and cations concentrate in the flow channel, although both species usually move in opposite directions, maintaining the electroneutrality. Thus, such a condition does not cause a driving force for liquid flows. This structure is crucial to generating an EHD flow whose flow speed reaches on the order of 1 mm/s in the channel because highly concentrated cations accelerated by external electric fields drag solvent molecules. EHD flows are observed and recorded by using a microscope and a high-speed camera as shown in **Figure 1**. Second, a concentration difference between two liquid phases separated by an ion-exchange membrane causes an electrically polarized condition to be generated crossing an ion-exchange membrane⁴⁰. In this study, we find the importance of a considerable waiting time to equilibrate ion distributions and a corresponding electric potential, which cause preferable conditions to apply to a body force in a liquid. Crossing the ion-exchange membrane, a weakly polarized condition is achieved. In such a condition, an externally applied electric field induces directional ion transport that generates a body force in a liquid, and as a result, the momentum transfer from the ions to the solvent develops an EHD flow.

As mentioned above, the present devices succeed in drastically decreasing the applied voltage difference to a few volts, and thus this method is can be used for aqueous solutions, although the conventional electrical charge injection methods required tens of kV and are limited to an application to non-aqueous solutions.

Protocol

1. EHD Flow Induced by Rectified Ion Transport

1. Development of a flow channel device to rectify ion transport pathways

1. Make a PTFE mold of the reservoir:
 1. Cut a 13 x 30 x 10 mm³ mold from a polytetrafluoroethylene (PTFE) block using a milling machine (see **Figure 2**). Alternatively, purchase a custom-made product.
 2. Adhere acrylic plates of 15 x 18 x 1 mm³ at both ends of the PTFE mold with a plastic adhesive, which will make slits in the reservoir to settle the bias electrodes. These parts can be cut out from a large plate or purchased.
 3. Adhere the acrylic plates of 13 x 30 x 1 mm³ at the top and bottom surfaces of the PTFE mold with a plastic adhesive to make planar surfaces for clear observation.
2. Mix a silicone elastomer base and curing agent in the ratio of 10:1 in a 50 mL tube and shake the tube by hand.
3. Settle the liquid PDMS in a vacuum vessel and degas it by using a rotary pump.
4. Remove the tube from the vessel. Pour the PDMS into a 40 x 50 x 24 mm³ plastic vessel to mold the outer shape of the reservoir and place the reservoir mold (see step 1.1.1) in it.
5. Bake the whole body of the liquid PDMS on a hotplate at 80 °C for about 4 h.
6. After the bake, isolate the PDMS reservoir from the PTFE mold and the outer vessel by hand. Make a slit across the center of the reservoir by using a surgical knife. This will be used to put the edges of an anion-exchange membrane (prepared in step 1.1.16) into it using tweezers.

NOTE: The PDMS reservoir is filled with electrolyte solutions later, as shown in **Figure 2**.
7. Obtain glass plates (made by special order) with a circular shape of 18 mm in diameter or in a square with 18 mm edges.
8. Wash the glass plates by soaking them in acetone, ethanol, and pure water (in that order) in an ultrasonication bath for 15 min each.
9. Blow any residual liquids away with an air gun or heat the glass plates with a hotplate for 5 min at about 473 K.
10. Using radio frequency sputtering, coat the glass surface with Cr or Ti exposed to Ar plasma for 1 min at 75 W and successively, deposit an Au thin film for 5 min at 75 W, setting the thickness at approximately 100 nm.

NOTE: Before coating the glass surface with the target metals, the samples were set in a vacuum chamber that was evacuated with a rotary pump and a molecular diffusion pump until the pressure decreased to 1 x 10⁻² Pa.
11. Solder a lead on the Au electrode surface using a soldering iron.

NOTE: The shape of the Au electrode may possibly be replaced by squares and helical wires, maintaining surface areas large enough to generate ionic currents.
12. With tweezers, set the glass plates coated with an Au thin film at both ends of the reservoir. These are the bias electrodes.
13. Cut an anion-exchange membrane into a rectangular shape of 20 x 18 mm² by using scissors. A surface area of 13 mm in width and 10 mm in height is exposed to a liquid. Here, a box cutter or surgical knife may also be used to cut the membrane.
14. Cut out a rectangular piece of 3 x 5.5 mm² from one edge of the membrane with scissors.

NOTE: The thickness of the anion-exchange membrane is 220 μm. The membrane is easily cut with scissors or a box cutter. The edges of the membrane are partly fixed with the slits in the chamber.
15. Solidify a PDMS block with a stainless rod of a 1 x 1 mm² cross-section in the same way as in steps 1.1.4 - 1.1.5, to create a flow channel that penetrates the membrane. Leave the construction overnight and then pull the stainless rod out of the PDMS block.
16. Cut the PDMS block with a square flow channel into a 3 x 6 x 4.5 mm piece (see **Figure 2**) using a surgical knife. Make slits along the outer edges, then attach it to the membrane within the rectangular cutout.

NOTE: The top face of the channel has to be set horizontally for a clear observation of the particles in the flow channel *via* the transparent wall.

2. Preparation of solutions and pretreatments for experiments

1. Prepare NaOH aqueous solutions at concentrations of 1×10^{-1} , 1×10^{-2} , and 1×10^{-3} mol/L by diluting the stock solution.
2. Make a dispersion of polystyrene particles of 2.93 μm on average in diameter in each of the NaOH solutions prepared in step 1.2.1 by setting the concentration to 4.2×10^{-3} vol%.
NOTE: The size of the tracer particles may be changed appropriately to improve observability.
3. Ultrasonicate the formatted anion-exchange membrane of $20 \times 18 \text{ mm}^2$ with a slit of $3 \times 5.5 \text{ mm}^2$ 2x for 10 min in pure water at a power of 100 W.
4. With tweezers, set the anion-exchange membrane with the PDMS flow channel into the PDMS reservoir. Fill the reservoir with 4 mL of NaOH solution using a micropipette.
NOTE: The membrane surface and flow channel are immersed in the solution, where the membrane surface exposed to the solution is at least 100x larger than the cross-section of the flow channel.
5. Apply an electric potential of 2.2 V by using a DC power source in forward and backward directions for 2 h each in series, to improve the conductivity of the membrane before observation.
6. Pull the Au electrodes out with tweezers. Remove the solution from the reservoirs using a micropipette.
7. Set new Au electrodes in the reservoirs with tweezers. Fill the reservoirs with 4 mL of NaOH solution using a micropipette. Start observations when the solution is equilibrated.
NOTE: It may take a few minutes of waiting time until the natural convection settles down, which can be judged by observing the behavior of tracer particles.

3. Experimental setup and measurement systems

1. Set the frame rate and the exposure time of a high-speed complementary metal-oxide-semiconductor (CMOS) camera to 500 fps and 1 ms, respectively.
NOTE: As shown in **Figure 1**, the experimental device is set on the stage of a microscope connected to a high-speed CMOS camera to record the particle motions. The view is magnified in a 15 in monitor with a 100X lens.
2. Remove any bubbles from the channel by inserting the tip of a micropipette into the channel end to push or pull out them, before applying an electric potential.
3. Externally apply an electric potential of 2.2 V to the Au bias electrodes. Simultaneously monitor the electrical responses by using a potentiostat or a DC power source with a digital multimeter.
NOTE: The voltage value is determined to be the upper limit, avoiding the water electrolysis that generates O_2 and H_2 bubbles in the solution.
4. Record the behavior of the tracer particles on the computer.
5. Measure an electric potential difference between both ends of the flow channel by using Au probe electrodes and a digital multimeter to confirm that the concentration gradient of ions triggers an EHD flow^{38,39}.
6. Determine the origin of the Cartesian coordinate system at the center of the channel.
NOTE: The x-axis is along the longitudinal direction of the flow channel, and the y- and z-axes are in the horizontal and vertical directions in the cross-section of the channel, respectively, as shown in **Figure 2**. The transparent PDMS channel allows liquid flows to be visualized along the x-axis. The view is focused on the xy plane at $z = 0$ by controlling the depth of focus. The flow data are independent of x in the test section except just near the inlet and outlet of the channel, and the observation point is set at approximately 0.75 mm downstream from the origin, such that $x = 0.75$, $y = 0$, and $z = 0$ mm.
7. After a single measurement (of 15 s), short-circuit the electrodes by connecting them to each other with a lead for 20 min until the solution is equilibrated.
8. Next, move the entirety of the solution to another vessel (e.g., a 10 mL sample bottle) and stir it with a micropipette.
9. Pour the stirred solution into the chamber again using a micropipette when iteratively performing the experiment.
NOTE: After observation, the EHD flow velocity is evaluated by using the particle image velocimetry (PIV) method³⁹, which can be done by using the appropriate software to trace the displacement of particles and numerically evaluate the velocity. A detailed explanation of PIV methods and how to use them is omitted here because PIV analyses have been widely used and the procedures of computations depend on the software and operating system that is being used.

2. Observation of Cation-induced EHD Flows

1. Development of experimental device

1. Form Au bias electrodes with a $26 \times 10 \text{ mm}^2$ surface on the bottom glass plate according to procedures similar to those previously described in steps 1.1.5 - 1.1.7.
2. Using radio frequency sputtering, coat a glass surface with Cr or Ti exposed to Ar plasma for 2 min at 75 W and deposit an Au thin film for 5 min at 75 W.
NOTE: This shape of electrode is determined in order to highly concentrate electric fields in the narrowest channel region. The ratio of the electrode surface, whose area of $10 \times 10 \text{ mm}^2$ is exposed to a liquid, to the cross-section of the channel is ideally 100:1; this ratio is predicted to be sufficient to drop the electric potential at the channel by a large amount¹⁶.
3. Solder a lead line at an edge of the electrodes by using a soldering iron.
4. From a large silicone rubber sheet, cut out 2 chambers, each made of a $1 \times 1 \times 1 \text{ mm}^3$ flow channel placed between two $10 \times 10 \times 1 \text{ mm}^3$ reservoirs, using a surgical knife (see **Figure 3**). These parts may be replaced by PDMS.
5. Cut out a cation-exchange membrane with an average thickness of 127 μm to $20 \times 30 \text{ mm}$ using a box cutter or surgical knife, as shown in **Figure 3**.
6. Ultrasonicate each part in pure water for 15 min by applying 100 W.

7. Insert a cation-exchange membrane between the chambers using tweezers, as shown in **Figure 3**. This will separate 2 electrolyte solutions of different concentrations.
8. Press and seal the stack of the chambers and cation-exchange membrane with glass plates whose dimensions are 26 mm in width and 38 mm long.

2. Preparation of solutions

1. Prepare a dispersion of polystyrene particles of an average diameter of 1.01 μm in a 1×10^{-2} mol/L tris(hydroxymethyl)aminomethane ethylenediaminetetraacetic acid (Tris-EDTA) buffer solution, where the volume ratio is adjusted to 1×10^{-2} vol%.
2. Prepare a mixture of 1 mol/L of KCl and 1×10^{-2} mol/L of Tris-EDTA.
3. Inject the Tris-EDTA/polystyrene particle and the Tris-EDTA/KCl solutions into the lower and upper chambers, respectively, via syringe needles inserted from the side walls of the chambers.

NOTE: The quantity of the solutions injected into each chamber is about 210 μL .

4. Wait for about 18 h until the solution is equilibrated as a result of a diffusion of the ions to relax the ion concentration difference between the upper and lower layers.

NOTE: In the diffusion process, K^+ in the upper solution and H^+ in the membrane are expected to penetrate the membrane first, and Cl^- is expected to follow them.

3. Experimental setup and measurement systems

1. Set the experimental device developed in step 2.1 on the stage of the inverted microscope by hand, as shown in **Figure 3**. Connect the microscope to a high-speed CMOS camera to monitor the trajectories of the particle motions and record the observation data on a computer.
2. Apply an electric potential difference of 2 V for 6 s between the two electrodes by using a function generator as a power source.
3. To confirm that EHD flows are induced by ion transport, measure the ionic currents simultaneously by using an ammeter⁴⁰.
4. Analyze the recorded trajectories of the particles by the particle tracking velocimetry (PTV) method³⁹.

NOTE: After the observations, the EHD flow velocity is evaluated by the PTV method, which is possible by using appropriate software, to trace the displacement of particles and numerically evaluate the velocity. A detailed explanation of PTV methods and how to use them is omitted here because PTV analyses have been widely used and the procedures of the computations depend on the software and operating system that is being used.

Representative Results

Figure 4 (video figure) presents a representative result of an EHD flow generation, resulting from the rectification of ion transport pathways and highly concentrated cations that induced a liquid flow in the channel, according to step 1 of the protocol. **Figure 5** shows a result of the PIV analysis, where 20 data points near the center of the channel ($y = z = 0$ mm) were averaged. In the case of the 1×10^{-1} mol/L NaOH solution, when an electric potential of 2.2 V was applied at $t = 5$ s, the velocity of the tracer particles quickly increased to a peak value. After that, the velocity decreased and converged to 0. The peak velocity reached a near 2 mm/s. This is a typical result of an EHD flow generated by using an anion-exchange membrane and a 1×10^{-1} mol/L NaOH solution.

It was also confirmed that the electrophoretic transport velocity of tracer particles was much lower than the peak velocity of the liquid flow in the 1×10^{-1} mol/L NaOH solution^{38,39}. As discussed in the literature³⁹, this kind of EHD flow is considered to consist of reversed flows dragged by OH^- passing through the membrane and Na^+ and H^+ concentrated in the flow channel to compensate for the anion transport in the membrane. As the concentration decreased, the transport behavior tended to become slower. This means that the duration-until the velocity reached a peak-and the decay time seemed to be longer, decreasing the peak value of the velocity. This result indicated that the number of ions whose motion was driven by electric forces decreased, and consequently, the electric body force in the liquid was also reduced.

One important observation is that continuous ionic currents rectified by the ion selective interfaces caused solvent molecules to be dragged in one direction and this caused a liquid flow to develop. In this case, there is a possibility that the liquid flow was enhanced by ion concentration polarization crossing the anion-exchange membrane that triggered the reverse flow in the channel. This point was already mentioned in a previous study³⁹. It was supposed that AC fields were also effective to control liquid flows periodically changing directions. The present EHD flow was limited to transient responses because of the finite number of Na^+ ions; this situation was not conducive to maintaining a steady cationic current, even though the applied voltage of 2.2 V was enough to induce the electrolysis of water. To generate constant EHD flows, we propose dragging solvent molecules with ion species that are the dominant carrier of the ionic current. Further details will be verified in our future work. Here, we introduced a representative result of an EHD flow that could be induced in NaOH solutions by rectifying ion transport pathways. Details about the concentration dependency and electric potential differences are also discussed by Yano, Doi, and Kawano^{37,38} and Yano, Shirai, Imoto, Doi, and Kawano³⁹.

Figure 6 (video figure) shows a representative result of the EHD flow generated in an electrically polarized solution under ionic current conditions. The velocity response of the EHD flow was also analyzed by tracking the tracer particles, as shown in **Figure 7**, which was a typical result obtained by tracking a single particle near the center of the flow channel. When an electric potential of 2 V was applied from $t = 2$ to 8 s, polystyrene particles responded to the applied electric field. At $t = 2$ s, the particle quickly translocated in the backward direction, corresponding to the electrophoretic transport of negative charges. After a short-time response, the flow changed to the forward direction and the velocity became steady at 30 $\mu\text{m/s}$ until the electric potential was turned off.

In this period, the negatively charged polystyrene particles moved in the direction of the transport of the positive charges. In general, the direction could not be reversed spontaneously under the one-directional electric field, even if the surface charge of the particles was fully shielded by the counter cations. Thus, this result indicated that cations dispersed in the solution were also electrophoretically transported along the electric fields, dragging solvent molecules that gradually developed a liquid flow. Negative charges highly concentrated on the particle surface caused an electric force stronger than that by cations distributed in the solution, and, thus, firstly drove the transport in the negative direction. After that, a liquid flow dragged by the cationic current increased a drag force on the particle. In this regime, velocity gradients were actually observed along the y -axis perpendicular to the flow direction, and, thus, a liquid flow generation was actually confirmed.

The behavior of polystyrene particles affected by EHD flows was also evaluated in a previous study, and it was found that the velocity of the EHD flow proportionally increased with an increasing ionic current. A waiting time of over 18 h before applying an external electric field is the most important factor for inducing a constant EHD flow, because it takes such a long time for the ion distributions to be equilibrated since they are almost uniform in the channel. As a result, Poiseuille-like flow patterns are steadily observed. On the other hand, we could not confirm a steady flow when the waiting time was not sufficient to achieve uniform ion distributions.

After observing a constant velocity, the electric potential was turned off at $t = 8$ s. Here, to quickly change the electric potential difference from 2 to 0 V, the shielded electrodes may require an excessive application of the electric potential to make both electrode surfaces equivalent. In that process, ions highly concentrated near the electrode surfaces receive repulsive electric forces, which result in reversed ionic currents. Especially, the cationic current that was dominant in the lower layer caused a liquid flow to be generated, and a transient response in the backward direction was actually observed in the experimental result, which immediately appeared when the electric potential was turned off and converged to 0 $\mu\text{m/s}$. Such processes in the EHD flow generation were typical in this experiment. Next to the steady EHD flow, the reverse flows observed when switching the electric potential on and off are also interesting. In the transient responses, electrochemical reactions at the electrode surfaces possibly cause drastic ion concentration gradients that induce the diffusion potential as well as externally applied electric potentials. Such complicated ion transport phenomena have not yet been clarified enough and, therefore, are subjects to be solved in future work.

The mechanisms of the EHD flow generation are schematically presented in **Figure 8**. An EHD flow induced in NaOH solutions is shown in **Figure 8a**, corresponding to the case of **Figure 4**. The EHD flow dragged by Na^+ in the channel is triggered by the transport of OH^- in an anion-exchange membrane. The unsteady flow is caused by the dissipation due to mass flux damping, momentum flux damping, surface mobility, and electrowetting of the electrode surfaces. Another mechanism of EHD flow induced under cationic current conditions, which are more dominant than anionic ones, is represented in **Figure 8b**. K^+ ions first penetrate a cation-exchange membrane, causing cation-dominant conditions, and, as a result, EHD flow is induced along the cationic current.

As described above, maintaining electrically polarized conditions under ionic current conditions by reducing the application of the electric potentials is key to generating steady EHD flows. By using the present methods, a few volts may be sufficient to induce EHD flows in aqueous solutions, although water electrolysis is necessary to maintain constant ionic currents to enhance the momentum transfer from electrolyte ions to solvent molecules.

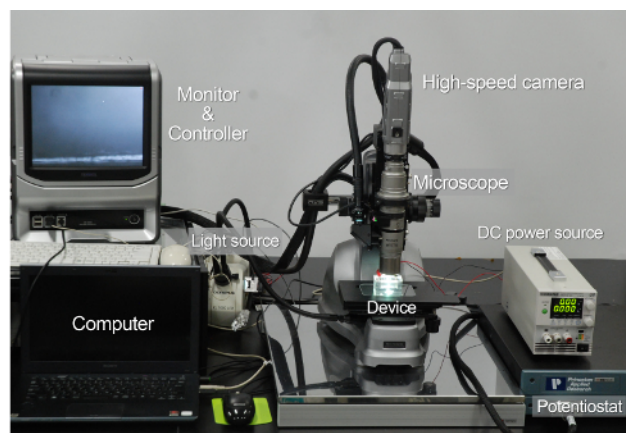


Figure 1: Photograph of experimental setup for EHD flow observation. Motions of tracer particles are traced by a microscope connected to a high-speed camera, recording the trajectories in the controller. Electric potentials are applied by using a potentiostat or a DC electric power source. [Please click here to view a larger version of this figure.](#)

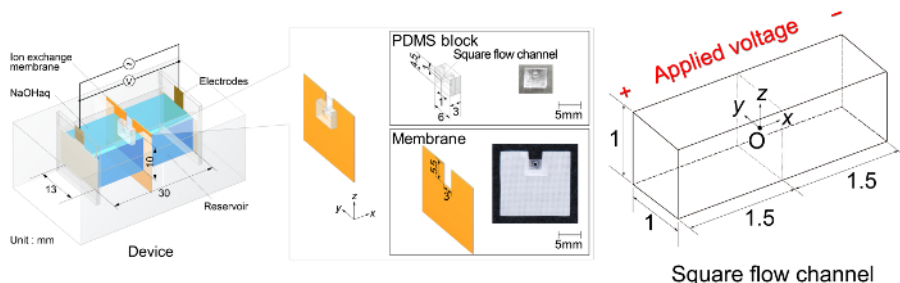


Figure 2: Schematic illustration of an experimental device. A flow channel made of PDMS is fixed in an anion-exchange membrane and filled with an NaOH aqueous solution. Au electrodes are placed at both ends of the solution. The origin of the coordinate is set at the center of the square flow channel and an observation area is in an xy plane near $x = 0.75$ and $z = 0$ mm. [Please click here to view a larger version of this figure.](#)

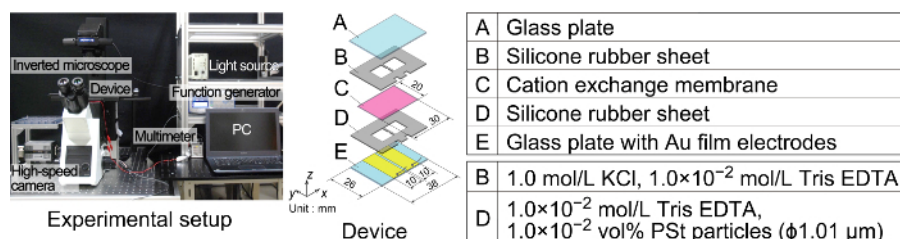


Figure 3: Photograph of experimental setup and schematic diagram of a device to induce a cation-dragged EHD flow in an electrically polarized solution. A 1 mol/L KCl and 1×10^{-2} mol/L Tris-EDTA buffer solution and a 1×10^{-2} vol% polystyrene (PSt) particle dispersion in a 1×10^{-2} mol/L Tris-EDTA buffer solution are separated with a cation-exchange membrane, where the average diameter of the PSt particles is 1.01 μm . [Please click here to view a larger version of this figure.](#)

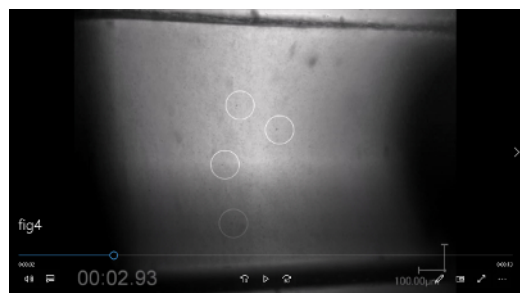


Figure 4 (video figure): A movie of EHD flow driven by the transport of Na^+ ions concentrated in the flow channel. The tracer particles are transported along the direction of the electric field when an electric potential of 2.2 V is applied at $t = 5$ s. Negatively charged polystyrene particles are brought to the cathode side in an EHD flow driven by the cationic current in the channel. In the case of a 1×10^{-1} mol/L NaOH solution, a peak velocity near 2 mm/s is reached quickly after applying an electric potential, and the velocity successively decays to zero. [Please click here to view this video.](#) (Right-click to download.)

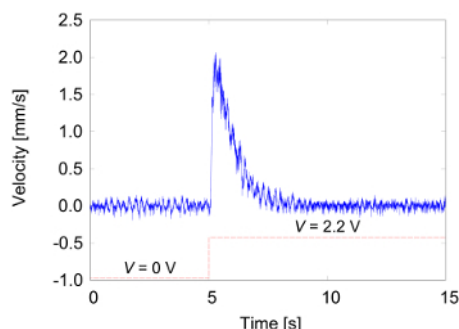


Figure 5: The response of EHD flow observed in the flow channel, resulting from the PIV analysis for the recorded movie of Figure 4. The velocity response (blue solid line) was obtained by the average of 20 points near the center of the channel ($y = z = 0$ mm). The velocity is quickly increased after applying an electric voltage of 2.2 V at 5 s and gradually converges to 0 mm/s. The sequence of the applied voltage is also shown with a red dashed line. [Please click here to view a larger version of this figure.](#)



Figure 6 (video figure): A movie of EHD flow observed in an electrically polarized solution, separating a 1 mol/L KCl solution and polystyrene dispersion by using a cation-exchange membrane. Applying an electric potential of 2 V from $t = 2$ to 8 s, the transport of tracer particles reflects an EHD flow driven by a cationic current. A constant flow velocity reaches $30 \mu\text{m/s}$ during the application of the potential. Additionally, the particles also briefly respond in the negative direction when the electric potential is turned on and off because the electrical charge of a particle firstly affects the motion. [Please click here to view this video.](#) (Right-click to download.)

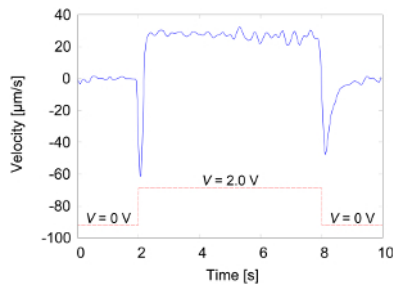


Figure 7: The response of EHD flow observed in the channel, resulting from the PTV analysis for the recorded movie of Figure 6. The velocity response (blue solid line) was obtained by tracking a single particle near the center of the channel. The sequence of the applied voltage is also shown with a red dashed line. [Please click here to view a larger version of this figure.](#)

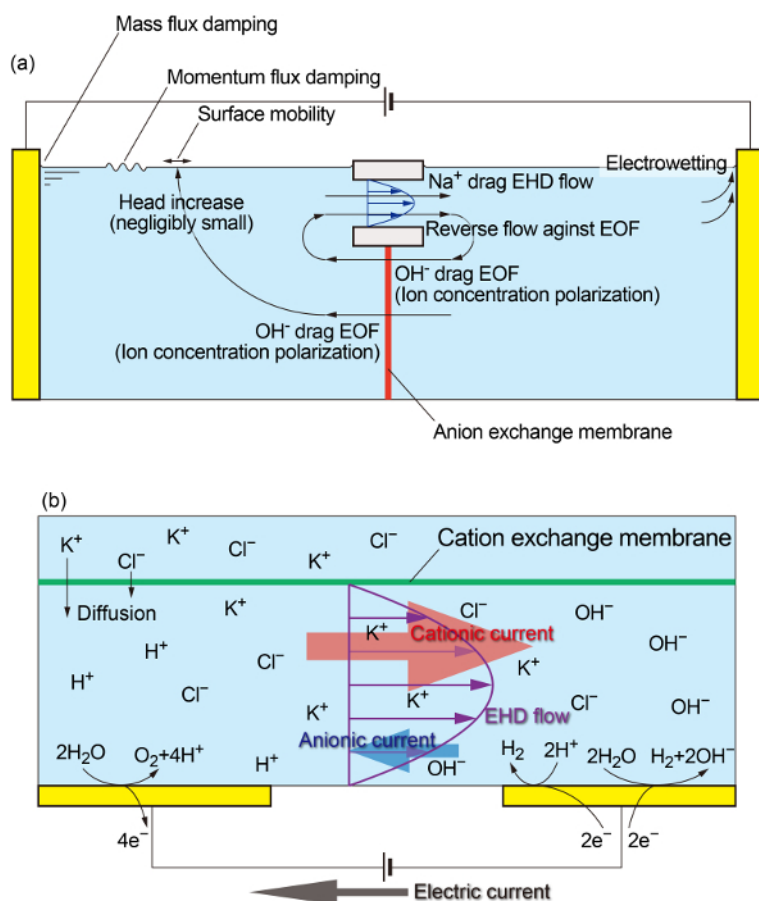


Figure 8: Schematics of EHD flow generation mechanisms corresponding to Figures 4 and 5 (panel a) and 6 and 7 (panel b). (a) Liquid flows are induced in an NaOH aqueous solution that is separated with an anion-exchange membrane, where EOF induced by an OH^- transport in the membrane triggers a flow dragged by an Na^+ transport in the channel and is partly dissipated with mass flux damping, momentum flux damping, surface mobility, and electrowetting of the electrode surfaces. (b) The cationic current is more dominant than the anionic current because K^+ firstly penetrates a cation-exchange membrane, which contributes to a liquid flow dragged by cations under constant current conditions involving water electrolysis. [Please click here to view a larger version of this figure.](#)

Discussion

The purpose of this study was to separate cations and anions in aqueous solutions in terms of spatial distributions and transport numbers. Using an anion-exchange membrane, the transport of anions and cations could be rectified in the membrane and in a flow channel that penetrates the membrane, respectively. Alternatively, a cation-exchange membrane that separated high and low concentration solutions worked to generate electrically polarized solutions after a considerable waiting time. As a result, rectified ionic currents succeeded in reducing the applied voltages to induce ion-dragged EHD flows.

The methods presented here are available for aqueous solutions with low application voltages in comparison to conventional methods that require extremely high voltages of tens of kV to inject electrical charges into non-polar solutions. It was clarified that EHD flows are effective in aqueous solutions as well as non-polar solutions.

However, the present methods depend on water electrolysis to maintain constant ionic currents in which the ideal potential of water electrolysis is known to be 1.23 V. Thus, there is a limitation on the applied voltage to avoid generating O_2 and H_2 bubbles that change the properties of a liquid. To overcome this limitation, materials of the electrodes and electrolyte solutions have to be appropriately determined to set electrochemical reactions at the electrode surfaces to generate ionic currents in the solutions. At every trial, the electrode surfaces should be polished and bared to make a strong electric field in the solution, enhancing the electrochemical reactions.

In this study, the use of ion-exchange membranes was proposed to rectify the transport pathways of ion species. On the other hand, the efficiency of EHD flow generation seemed to depend on the capability of the membranes. As discussed in the protocol, the diffusion of ions takes a considerable waiting time until it becomes stable. Therefore, the preprocess to increase the conductivity of the membranes is crucial to improving the efficiency of the EHD flow generation. When maintaining ionic current conditions in externally applied electric fields, transport properties of ions are improved, and electrically polarized conditions are effectively achieved.

In the future, EHD flows of aqueous solutions are expected to be applicable for liquid flow control systems in micro- and nanofluidic devices combined with EOFs and the like. Furthermore, applications for medical devices, in which ion transport has an important role to stimulate biological cells and signal transduction, are also challenging.

Disclosures

The authors have nothing to disclose.

Acknowledgements

The authors have no acknowledgments.

References

1. Stuetzer, O.M. Ion drag pressure generation. *Journal of Applied Physics*. **30**, 984-994 (1959).
2. Stuetzer, O.M. Ion drag pumps. *Journal of Applied Physics*. **31**, 136-146 (1960).
3. Melcher, J.R., Taylor, G.I. Electrohydrodynamics: A review of the role of interfacial shear stresses. *Annual Review of Fluid Mechanics*. **1**, 111-146 (1969).
4. Saville, D.A. Electrohydrodynamics: The Taylor-Melcher leaky dielectric model. *Annual Review of Fluid Mechanics*. **29**, 27-64 (1997).
5. Stein, D., Kruithof, M., Dekker, C. Surface-charge-governed ion transport in nanofluidic channels. *Physical Review Letters*. **93**, 035901 (2004).
6. Dekker, C. Solid-state nanopores. *Nature Nanotechnology*. **2**, 209-215 (2007).
7. Schoch, R.B., Han, J., Renaud, P. Transport phenomena in nanofluidics. *Reviews of Modern Physics*. **80**, 839-883 (2008).
8. Iverson, B.D., Garimella, S.V. Recent advances in microscale pumping technologies: A review and evaluation. *Microfluidics and Nanofluidics*. **5**, 145-174 (2008).
9. Sparreboom, W., van den Berg, A., Eijkel, J.C.T. Principles and applications of nanofluidic transport. *Nature Nanotechnology*. **4**, 713-720 (2009).
10. Venkatesan, B.M. Bashir, R. Nanopore sensors for nucleic acid analysis. *Nature Nanotechnology*. **6**, 615-624 (2011).
11. Uehara, S., Shintaku, H., Kawano, S. Electrokinetic flow dynamics of weakly aggregated λ DNA confined in nanochannels. *Journal of Fluids Engineering*. **133**, 121203 (2011).
12. Guan, W., Reed, M.A. Electric field modulation of the membrane potential in solid-state ion channels. *Nano Letters*. **12**, 6441-6447 (2012).
13. Yasui, T. *et al.* DNA manipulation and separation in sublitographic-scale nanowire array. *ACS Nano*. **7**, 3029-3035 (2013).
14. Ren, Y. *et al.* Particle rotational trapping on a floating electrode by rotating induced-charge electroosmosis. *Biomicrofluidics*. **10**, 054103 (2016).
15. Ren, Y. *et al.* Flexible particle flow-focusing in microchannel driven by droplet-directed induced-charge electroosmosis. *ELECTROPHORESIS*. **39**, 597-607 (2018).
16. Qian, W., Doi, K., Uehara, S., Morita, K., Kawano, S. Theoretical study of the transpore velocity control of single-stranded DNA. *International Journal of Molecular Sciences*. **15**, 13817-13832 (2014).
17. Qian, W., Doi, K., Kawano, S. Effect of polymer length and salt concentration on the transport of ssDNA in nanofluidic channels. *Biophysical Journal*. **112**, 838-849 (2017).
18. Liu, W. *et al.* A universal design of field-effect-tunable microfluidic ion diode based on a gating cation-exchange nanoporous membrane. *Physics of Fluids*. **29**, 112001 (2017).
19. Liu, W. *et al.* Control of two-phase flow in microfluidics using out-of-phase electroconvective streaming. *Physics of Fluids*. **29**, 112002 (2017).
20. Osman, O.O., Shintaku, H., Kawano, S. Development of micro-vibrating flow pumps using MEMS technologies. *Microfluidics and Nanofluidics*. **13**, 703-713 (2012).
21. Osman, O.O., Shirai, A., Kawano, S. A numerical study on the performance of micro-vibrating flow pumps using the immersed boundary method. *Microfluidics and Nanofluidics*. **19**, 595-608 (2015).
22. Daiguji, H. Ion transport in nanofluidic channels. *Chemical Society Reviews Home*. **39**, 901-911 (2010).
23. Ristenpart, W.D., Aksay, I.A., Saville, D.A. Assembly of colloidal aggregates by electrohydrodynamic flow: Kinetic experiments and scaling analysis. *Physical Review E*. **69**, 021405 (2004).
24. Ristenpart, W.D., Aksay, I.A., Saville, D.A. Electrohydrodynamic flow around a colloidal particle near an electrode with an oscillating potential. *Journal of Fluid Mechanics*. **575**, 83-109 (2007).
25. Schoch, R.B., Hann, J., Renaud, P. Effect of the surface charge on ion transport through nanoslits. *Physics of Fluids*. **17**, 100604 (2005).
26. Ross, D., Johnson, T.J., Locascio, L.E. Imaging of electroosmotic flow in plastic microchannels. *Analytical Chemistry*. **73**, 2509-2515 (2001).
27. Hsieh, S.-S., Lin, H.-C., Lin, C.-Y. Electroosmotic flow velocity measurements in a square microchannel. *Colloid and Polymer Science*. **284**, 1275-1286 (2006).
28. Rubinstein, I., Zaltzman, B. Electro-osmotically induced convection at a permselective membrane. *Physical Review E*. **62**, 2238-2251 (2000).
29. Bard, A.J., Faulkner, L.R. *Electrochemical methods*, 2nd ed. 362-363, John Wiley & Sons, Danvers, MA (2001).
30. Brask, A., Goranović, G., Jensen, M.J., Bruus, H. A novel electro-osmotic pump design for nonconducting liquids: theoretical analysis of flow rate-pressure characteristics and stability. *Journal of Micromechanics and Microengineering*. **15**, 883-891 (2005).
31. Takamura, Y. *et al.* Low-voltage electroosmosis pump for stand-alone microfluidics devices. *Electrophoresis*. **24**, 185-192 (2003).
32. Zeng, S., Chen, C.-H., Mikkelsen, J.C., Santiago, J.G., Fabrication and characterization of electroosmotic micropumps. *Sensors and Actuators B: Chemical*. **79**, 107-114 (2001).
33. Bhaumik, S.K., Roy, R., Chakraborty, S., DasGupta, S. Low-voltage electrohydrodynamic micropumping of emulsions. *Sensors and Actuators B: Chemical*. **193**, 288-293 (2014).
34. El Moctar, A.O., Aubry, N., Batton, J. Electro-hydrodynamic micro-fluidic mixer. *Lab on a Chip*. **3**, 273-280 (2003).

35. Bart, S.F., Tavrow, L.S., Mehregany, M., Lang, J.H. Microfabricated electrohydrodynamic pumps. *Sensors and Actuators A: Physical*. **21**, 193-197 (1990).
36. Ashikhmin, I.A., Stishkov, Y.K. Effect of insulating walls on the structure of electrodynamic flows in a channel. *Technical Physics*. **57**, 1181-1187 (2012).
37. Yano, A., Doi, K., Kawano, S. Observation of electrohydrodynamic flow through a pore in ion-exchange membrane. *International Journal of Chemical Engineering and Applications*. **6**, 254-257 (2015).
38. Doi, K., Yano, A., Kawano, S. Electrohydrodynamic flow through a 1 mm² cross-section pore placed in an ion-exchange membrane. *The Journal of Physical Chemistry B*. **119**, 228-237 (2015).
39. Yano, A., Shirai, H., Imoto, M., Doi, K., Kawano, S. Concentration dependence of cation-induced electrohydrodynamic flow passing through an anion exchange membrane. *Japanese Journal of Applied Physics*. **56**, 097201 (2017).
40. Nagura, R., Doi, K., Kawano, S. Characterisation of microparticle transport driven by ionic current conditions in electrically polarized aqueous solutions. *Micro & Nano Letters*. **12**, 526-531 (2017).
41. Doi, K., *et al.* Nonequilibrium ionic response of biased mechanically controllable break junction (MCBJ) electrodes. *The Journal of Physical Chemistry C*. **118**, 3758-3765 (2014).